View metadata, citation and similar papers at core.ac.uk
brought to you by CORE
provided by NASA Technical Reports Server

MONTE CARLO SIMULATION OF E.A.S. GENERATED BY 10^{14}-10^{16} eV PROTONS

Fenyves, E.J. and Yunn, B.C.
University of Texas at Dallas
P.O. Box 830688
Richardson, TX 75083-0688

Todor Stanev
Bartol Research Foundation of the Franklin Institute
University of Delaware
Newark, DE 19716

1. Introduction

Detailed Monte Carlo simulations of extensive air showers to be detected by the Homestake Surface-Underground Telescope (1) and other similar detectors located at sea level and mountain altitudes have been performed for 10^{14}-10^{16} eV primary energies. The results of these Monte Carlo calculations will provide an opportunity to compare the experimental data with different models for the composition and spectra of primaries and for the development of air showers (2).

In the present paper we report on the results obtained for extensive air showers generated by 10^{14}-10^{16} eV primary protons.

2. Monte Carlo Simulation of the Hadronic Cascade

The interaction model used assumed inelastic cross sections increasing with energy as $\ell n^{1.8} s$, which corresponds to a $\ell n^2 s$ rise of the inelastic p-p cross section. The x distribution obeys radial scaling and is realized through the splitting technique suggested by A.M. Hillas. The K/π ratio is 0.09 and energy independent.

Transverse momentum distribution is of the form $p_\perp \exp(-Kp_\perp)$ and includes the "sea gull" effect. For $x < 0.2$, $K = \frac{2}{x + 1/4}$, while for $x > 0.2$ we used a constant exponent of -4.44 for pions.

The secondary particles are followed until they reach certain threshold energy levels: 1.7 TeV for muons, 0.01 and 0.1 TeV for electrons, gammas, and 0.1 TeV for hadrons.

3. Simulation of the Electromagnetic Cascades

The electromagnetic cascades generated by gammas and electrons are propagated to the height of detection by applying the parametrized analytical formulas for the longitudinal development and lateral distribution of the electron component obtained by Fenyves and Yunn in previous Monte Carlo simulations of electromagnetic cascades (3). The threshold energy levels for the electromagnetic cascade generating gammas and electrons were: 0.01 TeV for 10^{14} and 10^{15} eV primary protons, and 0.1 TeV for 10^{16} eV protons. The average number of gammas and electrons above the threshold per shower is given in Table 1. (Muons above 1.7 TeV are also included in the Table.)

Table 1

E_p(eV)	N_γ	N_e	N_μ
10^{14}	361 ± 8	3.9 ± 0.3	0.30 ±0.06
10^{15}	2612 ±61	31.9 ± 1.1	1.54 ±0.17
10^{16}	3015 ±78	34.9 ± 1.2	8.20 ±0.50

From the extrapolation of the gamma spectra below the threshold levels correction factors were calculated for the missing low energy electromagnetic cascades. The correction factors for the total number of electrons of the air shower are dependent on the depth and the primary proton energy varying between 1.010 and 1.021.

The geomagnetic effect was included in the calculation by stretching the east-west axis of each vertical electromagnetic cascade by $[1 + 0.05(\cos\lambda/P)^2]^{\frac{1}{2}}$ where λ is the geomagnetic latitude and P the pressure in atmospheres (4). The individual cascades were then folded together to form the electron component of the extensive air shower.

4. Results

We have run a total of 220 extensive air showers generated by 10^{14}, 10^{15} and 10^{16} eV primary protons in a standard atmosphere. As expected the longitudinal development of these showers could not be approximated well with the standard formula used for the electron component of electromagnetic cascades generated by single gammas (3)

$$N_e(E_o,E,t)= \frac{A(E,s)0.31}{\sqrt{y}} \exp\,[t(1-1.5\,\ell n\, s)] \qquad (1)$$

where t is the depth measured in radiation lengths (37.1 g/cm^2), $y = \ell n\, E_o/\varepsilon_o$ (ε_o= 81 MeV),

$$s = \frac{3t}{t + 2y} \qquad (2)$$

and A(E,s) is the fraction of electrons having energies larger than the electron threshold energy, E. (E=5MeV and A(5MeV,s)=0.67 were used in the present study (3).)

We could, however, fit N_e^{max} and t_{max} calculated from Eq.(1) simultaneously to the corresponding average values obtained for the 10^{14}, 10^{15} and 10^{16} eV showers by varying E_o, the energy of the cascade generating gamma. The longitudinal development of the simulated air showers was, however, increasing faster before t_{max}, and decreasing slower after t_{max} than the values calculated from Eq.(1). This is expected because the electromagnetic component of the air shower starts with a large number of gammas, and dies out slower after the maximum due to new electromagnetic cascades generated by the hadronic core.

According to this we modified Eqs.(1) and (2) simply by replacing t in both equations by

$$t' = t + \beta(t_{max} - t)t^{\gamma} \qquad (3)$$

where β and γ are constants depending on the primary proton energy, and the second term increases or decreases the effective t' values as compared to t before or after the maximum, respectively.

The optimum E_o, β and γ values obtained for this parametrization for E_p=10^{14}, 10^{15} and 10^{16} eV are given in Table 2. Fig. 1 shows the good agreement between the Monte Carlo simulated average values (dots with error bars) and the smooth curves calculated by using Eqs.(1) and (2) modified by Eq.(3) with the parameter values given in Table 2.

Table 2

E_p(eV)	E_o(eV)	β	γ
10^{14}	$5.2 \cdot 10^{13}$	0.0100	1.00
10^{15}	$6.4 \cdot 10^{14}$	0.0173	0.75
10^{16}	$6.9 \cdot 10^{15}$	0.0300	0.50

Eqs.(1), (2) and (3) can also be used to describe moderately inclined showers ($\theta \leq 30^o$). Then t in Eq.(3) is the slant depth measured from the top of the atmosphere. The energy of the single gamma, E_o, simulating the longitudinal development of the air shower is increasing with E_p, the energy of the shower as expected because of the increasing probability of charged pions and kaons to produce nuclear interactions rather than decay. The β and γ values can be easily interpolated for intermediate E_p values when plotted on a log-log or lin-log scale vs. E_p, respectively.

The lateral distribution of electrons of air showers generated by 10^{14}, 10^{15} and 10^{16} eV protons was compared with the modified NKG formula

$$f(\frac{r}{r'_M}) = C(s) \, (\frac{r}{r'_M})^{s-2} \, (\frac{r}{r'_M} + 1)^{s-4.5} \qquad (4)$$

where r'_M is about half of the Molière length length, r_M, as suggested by A. M. Hillas (5), and s is calculated by Eq.(2) modified by Eq.(3) with the parameters given in Table 2. A good agreement was found for not too large distances from the core, from r=1m to about 300m, as illustrated in Figs. 2, 3 and 4 for 850 g/cm^2, the height of the Homestake Telescope where r'_M=45m (3). Similarly good agreement was found for other heights too. At larger distances from the core, however, even the modified the NKG formula fails to agree with the Monte Carlo simulated data. Corrections for this effect will be discussed in a forthcoming paper.

The geomagnetic effect is relatively small at sea level but increasing with altitude. The east-west axis of vertical showers is stretched by a factor of 1.013 at sea level, and 1.019 at 850 g/cm^2. The relative difference between the $f(r/r'_M)$ values averaged in a cone $\pm 45^o$ around the east-west axis and in a cone $\pm 45^o$ around the north-south axis is increasing with r from about -0.015 at r=1m, to about -0.075 at r=1000m.

5. Acknowledgements

The authors are indebted to N. R. Davis, S. S. Liao and D. J. Suson for their valuable cooperation. This work has been supported by the National Science Foundation.

References

(1) Cherry, M.L. et al., (1981), 17th Int. Cosmic Ray Conf., Paris, 11, p. 421.
(2) Fenyves, E.J. and Cherry, M.L., (1983), Proc. Cosmic Ray Workshop, Utah, p.173.
(3) Fenyves, E.J., Lee, C.J. and Yunn, B.C., (1983), 18th Int. Cosmic Ray Conf., Bangalore, 11, p. 240.
(4) Greisen, K., (1956), Progr. in Cosmic Ray Phys., Vol. III, p.1.
(5) Hillas, A.M., (1983), private communication.

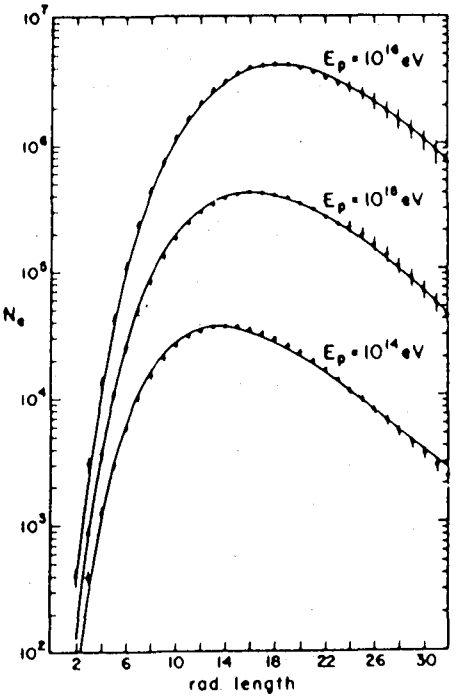

Fig. 1

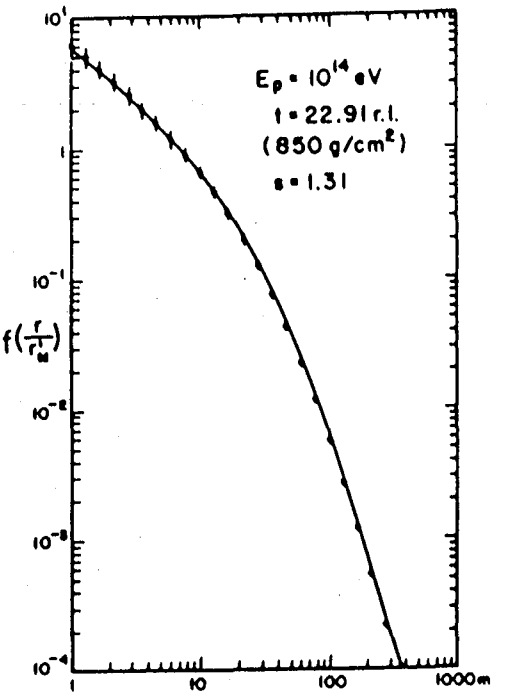

Fig. 2

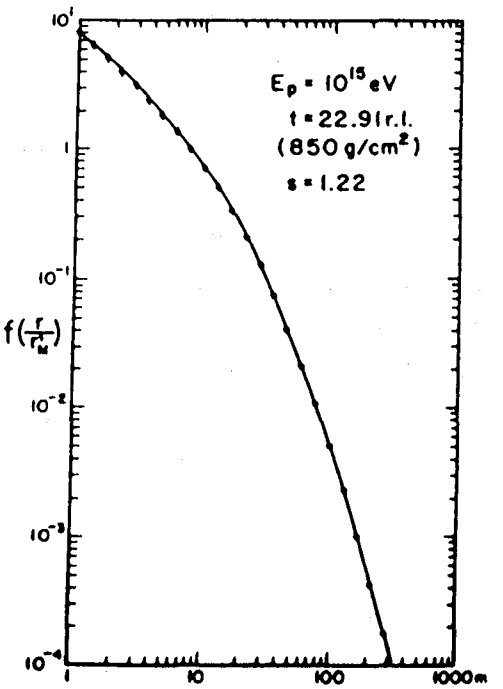

Fig. 3

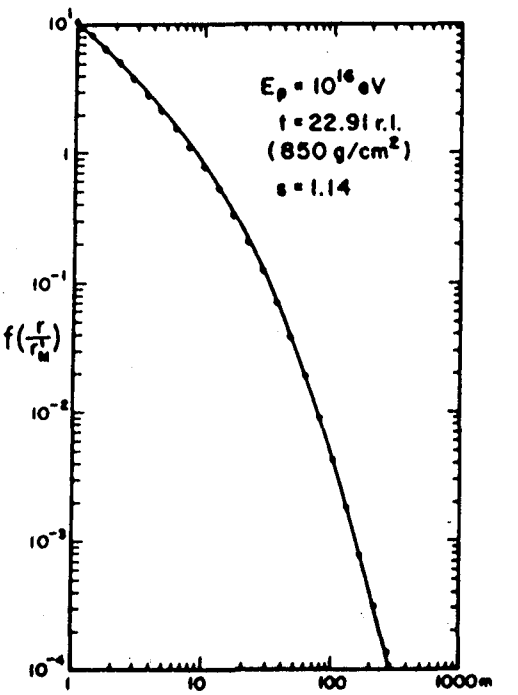

Fig. 4